Applied Catalysis B: Environmental 117–118 (2012) 105–117

Contents lists available at SciVerse ScienceDirect

Applied Catalysis B: Environmental

journal homepage: www.elsevier.com/locate/apcatb

Catalytic hydrotreatment of fast-pyrolysis oil using non-sulfided bimetallic Ni-Cu catalysts on a δ-Al_2O_3 support

A.R. Ardiyanti[a], S.A. Khromova[b], R.H. Venderbosch[c], V.A. Yakovlev[b], H.J. Heeres[a,*]

[a] Chemical Engineering, University of Groningen, Nijenborgh 4, 9747 AG, Groningen, The Netherlands
[b] Boreskov Institute of Catalysis, 5, pr. Akad. Lavrentieva, 630090 Novosibirsk, Russia
[c] BTG Biomass Technology Group BV, Josink Esweg 34, 7545 PN Enschede, The Netherlands

ARTICLE INFO

Article history:
Received 20 June 2011
Received in revised form
20 December 2011
Accepted 22 December 2011
Available online 12 January 2012

Keywords:
Hydrotreatment
Hydrodeoxygenation
Fast pyrolysis oil
Bio-oil
Anisole
Nickel catalyst
Characterization
Bimetallic nickel-copper catalysts

ABSTRACT

Fast pyrolysis oil from lignocellulosic biomass is an attractive energy carrier. However, to improve the product characteristics such as a reduced polarity and higher thermal stability, upgrading is required. We here report activities on the catalytic hydrotreatment of fast pyrolysis oil using bimetallic NiCu/δ-Al_2O_3 catalysts with various Ni/Cu ratios (0.32 to 8.1 w/w) at a fixed total metal intake of about 20 wt% with the objective to improve product properties for co-feeding applications in conventional oil refineries. Hydrotreatment reactions were initially carried out for a model compound (anisole, continuous set-up, 300 °C, 10 bar) and subsequently for fast pyrolysis oil (batch autoclave, 1 h at 150 °C followed by 3 h at 350 °C, at 100 bar initial pressure). Best results, i.e. the highest hydrodeoxygenation yield for experiments with anisole (75 mol%), and an upgraded oil with the most favorable properties for fast pyrolysis oil (high H/C ratio, low M_w of 500 g/mol, low thermogravimetric residue of 6.8 wt%), were obtained for a catalyst with a Ni to Cu wt% ratio of eight (16Ni2Cu). For this catalyst, hydrogen consumption was the highest (146 NL/kg_{PO}). The findings were rationalized using a reaction network model earlier developed for Ru/C. Analysis of catalyst (ICP, HRTEM, XRD and TGA) before and after reaction showed the occurrence of leaching of both active metals (Ni and Cu) and support, as well as coke deposition on the support. The most active catalyst in the series (16Ni2Cu) also gave lowest leaching and coking levels in the series.

1. Introduction

Fast pyrolysis is considered an attractive thermo-chemical technology to convert a solid biomass to a liquid energy carrier. The product, referred to as "fast pyrolysis oil" or "bio-oil", however, has a limited number of applications yet, such as the use as a boiler feed, co-feed in power plants or for the generation of electricity [1]. An interesting outlet for fast pyrolysis oil is the use as a co-feed in existing refinery units. This enables partial substitution of the fossil carbon in liquid transportation fuels by renewable carbon from biomass in existing infrastructure [2]. Unfortunately, fast pyrolysis oil cannot be used for co-feeding purposes. It is immiscible with typical petroleum feeds (such as vacuum gas oil) due to the presence of polar components, but moreover, it is highly acidic due to the presence of organic acids (up to 10 wt%) [3], leading to corrosion issues and possibly detrimental effects on the zeolitic catalysts in the FCC process [4], and has a strong tendency for coking at elevated temperatures.

Catalytic hydrotreatment is considered a versatile upgrading technology to improve the product properties of fast pyrolysis oil and to make it suitable for co-refining. In this approach, fast pyrolysis oil is reacted with hydrogen in the presence of a heterogeneous catalyst. Catalytic hydrotreatment is also commonly known as "hydrodeoxygenation" (HDO), though recent findings indicate that many other types of reactions occur, e.g. hydrogenation, hydrogenolysis and (hydro)-cracking. Typically, elevated pressures and temperatures (175–400 °C, 100–300 bar) are required. Catalytic hydrotreatment has been researched extensively [5] with crude pyrolysis oil [6,7] or model compounds [8–14] as the feedstock.

Commonly applied catalysts for the hydrotreatment of pyrolysis oil are typical hydrodesulfurization catalysts such as (sulfided) $NiMo/Al_2O_3$, $CoMo/Al_2O_3$, and $NiMo/Al_2O_3$-SiO_2 [15,16]. To cope with the harsh conditions, carbon-supported CoMo [15], Mo supported on TiO_2, ZrO_2 and TiO_2–ZrO_2 mixed oxides [8,12,16] have been tested as well. The latter catalysts all require sulfur in the feed to maintain activity. Pyrolysis oils contain only limited amounts of sulfur [17,18] and sulfur addition would be required during processing to maintain catalytic activity, which is not preferred for an environmental point of view.

Non-sulfided, non-noble metal catalysts have been tested for fast pyrolysis oil (model components) as well. Examples are non-sulfided Ni/SiO_2 catalyst for hydrodeoxygenation of phenol [17] and ZSM-5 catalyst for anisole [18,19]. Noble metal based catalysts

* Corresponding author. Tel.: +31 503634174.
E-mail address: h.j.heeres@rug.nl (H.J. Heeres).

0926-3373/$ – see front matter © 2012 Elsevier B.V. All rights reserved.
doi:10.1016/j.apcatb.2011.12.032

have also been explored. Examples are Pd on zeolites [19,20], Pd on CeO_2 and ZrO_2 [13], Pd/C and Pt/C [20,21], and Rh on zirconia [22]. Hydrotreatment of pyrolysis oil over Ru/C, yields product oils with a range of oxygen contents [2,20,23–25], the lowest values are around 5 wt%. Unfortunately, noble metal catalysts are very expensive and this may limit their application potential.

Most studies aim at the upgrading of fast pyrolysis oil to a liquid transportation fuel with properties mimicking that of typical hydrocarbon fuels (low oxygen content, H/C ratio between 1.8 and 2), and not for co-feeding purposes. Recently investigations have been reported on the co-processing of hydrotreated pyrolysis oils obtained with a Ru/C catalyst (oxygen contents > 5 wt%) in a lab scale simulated FCC unit (MAT) [2]. The hydrotreated products were successfully dissolved and processed in Long residue (20 wt% upgraded oil). The yields of FCC gasoline (44–46 wt%) and Light Cycle Oil (23–25 wt%) were close to the base feed and an excessive increase of undesired coke and dry gas was not observed. Experiments with undiluted upgraded oils were less successful and dry gas and coke yield were significantly higher than in case of co-feeding. This clearly demonstrates that co-processing is necessary to obtain good product yields. This study also shows that, in contrast to initial thoughts, it is likely not necessary to aim for an upgraded oil with an oxygen content lower than 1 wt%. Improved thermal stability of the upgraded oil to avoid charring during feeding or thermal processing and a low acidity to avoid corrosion are likely much more important.

In this study we report the use of bimetallic NiCu catalysts for the catalytic hydrotreatment of pyrolysis oil. Ni is a cheap metal compared to noble metals and is known for its high hydrogenation activity for a broad range of organic groups [26,27]. Cu is applied as a promoter, primarily to reduce the reduction temperature of Ni [28], and to prevent excessive carbon deposition on Ni [29]. δ-Al_2O_3 was used as the support as it is considered thermally more stable and less acidic than γ-Al_2O_3, the latter relevant in limiting coke formation [30,31]. Initial screening studies on the NiCu showed its potential for ethane hydrogenolysis [26] and vegetable oil hydrodeoxygenation [32]. To the best of our knowledge, the use of Ni-Cu catalysts for pyrolysis oil upgrading has not been investigated before. The effect of Ni to Cu ratio on catalyst performance was explored in detail, for a model component (anisole) and for typical fast pyrolysis oils. For comparison, experiments with a commercial Ru/C will be used as a benchmark, and product properties of the upgraded oil with the Ni-Cu catalysts are compared with those obtained using Ru/C. Catalysts were characterized before and after reaction to determine changes in morphology during reaction and to gain insights in catalyst stability.

2. Experimental

2.1. Materials

Anisole (99%, ACROS Organics, Geel, Belgium) was used as received. Fast pyrolysis oil (pine wood) was provided by VTT (Espoo, Finland). Relevant properties of the fast pyrolysis oil are given in Table 1. Ru/C (5 wt% of ruthenium, S_{BET} of 717 m^2/g, surface weighted Ru mean diameter (D[3,2]) of 6.8 μm) was obtained from Sigma–Aldrich. Hydrogen (>99.99% purity) was purchased from Hoekloos (Schiedam, The Netherlands). Spherical δ-Al_2O_3 particles with a diameter of 1.5 mm were obtained from Sasol (Hamburg, Germany).

2.2. Catalysts preparation

The δ-Al_2O_3 support was calcined in air at 1000 °C before impregnation. The BET surface area was about 110 m^2/g after the calcinations step. The metals were loaded by wet impregnation of the support with aqueous solutions of the metals salts ($Ni(NO_3)_2$ and $Cu(NO_3)_2$. After impregnation, the catalysts were dried at 100 °C for 12 h and subsequently crushed and sieved. The fraction 0.25–0.5 mm was used for the reactions. Before reaction, the catalysts were activated by reduction using hydrogen gas (vide infra).

Table 1
Relevant properties of the fast pyrolysis oil used in this study.

Element	Amount (wt%)
C (wet basis)	40.1
H (wet basis)	7.6
N (wet basis)	0.1
O (by difference, wet basis)	52.1
O (dry basis)	40.1
Water content	23.9
Atomic O/C (dry basis)	0.56
Atomic H/C (dry basis)	1.47

2.3. Catalysts characterization

Temperature programmed reduction (TPR). Catalyst samples (0.05 g) were placed in a quartz reactor (U-tube) and treated in a reducing atmosphere (10% H_2, 90% Ar at a flow rate of 20 ml/min, 1 atm) with a constant heating rate of about 8 °C/min until 800 °C. The hydrogen concentration in the outlet stream during reduction was measured by a thermal conductivity detector (TCD).

X-ray diffraction. XRD analyses were performed on a D500 Siemens (Germany) X-ray diffractometer using Cu Kα radiation. Diffraction patterns were recorded by scanning with 0.05° increments at an angle range from 30° to 80° using an accumulation period of 5 s per measurement. High temperature in situ XRD experiments were performed in a reactor chamber developed at the Boreskov Institute of Catalysis [33]. The hydrogen flow was set at 600 cm^3/min and a heating rate of 25 °C/min was applied. The pressure was 1 bar. The samples were heated in the hydrogen atmosphere to 300 °C. Then XRD patterns were recorded by scanning 2θ angles from 30° to 55° at 300 °C until the sample achieved quasi equilibrium as evident from the absence of noticeable changes in the diffraction patterns. Then the samples were cooled under a hydrogen atmosphere and the XRD patterns were recorded. The average sizes of the metal crystallites were calculated using the Scherrer equation [34]. For the Ni_x-Cu_{1-x} metal clusters, the composition of the clusters is calculated based on a known correlation between the Ni-Cu lattice parameter and the composition, as reported previously by Sinfelt et al. [26]. The lattice parameters were determined experimentally (vide infra).

High resolution transmission electron microscopy (HRTEM). TEM investigations were carried out on a JEM-4000EX transmission electron microscope at 200 kV accelerating voltage.

2.4. Catalytic hydrotreatment experiments using anisole

Catalytic hydrotreatment reactions of anisole were carried out in a continuous fixed bed reactor (internal diameter 5 mm) made of stainless steel at isothermal conditions (300 °C) and a total pressure of 10 bar. The reactor was packed with 0.5 ml of catalyst diluted with 1 ml of quartz sand (0.25–0.5 mm fraction). Prior to reaction, the catalyst was reduced in situ by flowing H_2 at the temperature of 300 °C, and 10 bar of H_2 pressure. After the reduction step, the reaction was started by feeding hydrogen and argon to the reactor with rates of 10 L/h each. Anisole was fed to the reactor with a WHSV in the range of 3–6 $kg_{liquid}/(kg_{cat}\ h)$. For a proper comparison of catalysts activities, feed rates of the reactants were selected in such a way that anisole conversions were less than quantitative.

Liquid products (organics and water) were collected in a trap cooled with ice.

2.4.1. Analysis of reaction products from the hydrotreatment of anisole

GC–FID. *GC–FID* was applied to analyze the organic phase of the liquid product. The analysis was carried out using a Hromos GH-1000 equipped with a split injector (300 °C), a FID detector (300 °C) and a capillary column (Zebron ZB-1, stationary phase 100% dimethylpolysiloxane, 0.25 μm × 0.32 mm × 30 m).

GC–TCD. GC–TCD was used to analyze the gas phase products. The analysis was carried out using a Hromos GH-1000 equipped with a packed column (stationary phases consisting of Silohrom and activated carbon).

2.4.2. Catalyst performance measures for hydrotreatment experiments using anisole

The conversion of anisole is defined as:

$$X_A = 1 - \frac{C_a}{C_a^0} \quad (1)$$

where C_a^0 and C_a are inlet and outlet concentrations of anisole, respectively. The extent of deoxygenation is defined as:

$$\text{HDO} = \frac{\sum_i C_i'}{\sum_i C_i} \times 100\% \quad (2)$$

where C_i' is the concentration of an oxygen-free product *i*, and C_i the concentration of product *i*. The selectivity for product *j* is defined as:

$$\text{Selectiviy} = \frac{C_j}{\sum_i C_i} \times 100\% \quad (3)$$

The total yield of oxygen-free HDO products is then defined as:

$$\text{Yield} = \text{HDO} \cdot X_A \quad (4)$$

Finally, the specific catalytic activity is defined as the rate of formation of oxygen-free products (mol h^{-1}) divided by the total amount active metals (Ni and Cu, g) in the catalyst sample.

2.5. Catalytic hydrotreatment reactions with fast pyrolysis oil

The hydrotreatment reactions with fast pyrolysis oil were performed in a 100 ml Parr reactor equipped with an overhead stirrer. The reactor was filled with 1.25 g of catalyst, which was pre-reduced at 10 bar of H_2 at 350 °C for 1 h. After reduction, the reactor was cooled to room temperature and 25 g of fast pyrolysis oil was injected. The reactor was then flushed with H_2, and subsequently pressurized with additional H_2 up to 100 bar (120 bar for Ru/C). The reactor was operated for 1 h at 150 °C, while being stirred at 1300 rpm, and subsequently the temperature was increased to 350 °C. The reactor was operated at 350 °C for another 3 h, where after the reactor was cooled to room temperature. This '2-stage' heating profile was performed to reduce the tendency for coke formation [5]. The results were compared with data obtained for Ru/C, an extensively studied catalyst for pyrolysis oil upgrading [2,20,25]. A sample from the gas phase was taken at room temperature and analyzed with GC–TCD. The reactor was opened, and the product phase was collected, centrifuged to separate the aqueous phase, organic phase, and solids (including the spent catalyst). The weight of all phases was determined for mass balance calculations. The organic phase was analyzed using various techniques (Section 2.4.1). The solid was thoroughly washed with acetone, dried, and characterized.

2.5.1. Analysis of the reaction products from the catalytic hydrotreatment of pyrolysis oil

GC–TCD. The gas phase from each experiment was analyzed using GC–TCD. A HP5890 Series II GC equipped with a CP Porabond Q (50 m × 0.5 mm, film thickness 10 μm) and a CP-Molsieve 5A (25 m × 0.53 mm, film thickness 50 μm) column was used for this purpose. The injector temperature was set at 150 °C and the detector temperature at 90 °C. The oven temperature was kept at 40 °C for 2 min, then increased to 90 at 20 °C/min, and kept at this temperature for 2 min. Helium was used as the carrier gas.

Elemental analysis. The liquid organic phase was analyzed by elemental analysis using a EuroVector EA3400 Series CHNS-O with acetanilide as the reference. The composition of oxygen was determined by difference. All analyses were carried out at least in duplicate and the average values are provided.

Water content. The water content of the liquid organic phases was determined using a Karl-Fischer (Metrohm 702 SM Titrino) titration. About 0.01 g of sample was introduced to an isolated glass chamber containing Hydranal solvent (Riedel de Haen). The titration was carried out using Hydranal titrant 5 (Riedel de Haen).

Thermogravimetric analysis (TGA). TGA data of the liquid organic phases were determined using a TGA 7 from PerkinElmer. The samples were heated in a nitrogen atmosphere with a heating rate of 10 °C/min and a temperature range between 20 and 900 °C.

Gel permeation chromatography. GPC analyses of the organic liquid phases were performed using an Agilent HPLC 1100 system equipped with a refractive index detector. Three columns in series of mixed type E (length 300 mm, i.d. 7.5 mm) were used. Polystyrene was used as a calibration standard. The organic phases were dissolved in THF (10 mg/mL) and filtered (pore size 0.2 μm) before injection.

GC–MS/FID. GC–MS/FID measurements on fast pyrolysis oil and the upgraded oils were performed at the von-Thunen Institute (Hamburg, Germany). All GC analyses were carried out on an Agilent 6890 systems coupled with parallel FI and MS detectors. Electron impact mass spectra were obtained using a 70 eV ionization energy. The GC split was 1:15, the injector temperature was 250 °C, and an injection volume of 1 μl was applied. The temperature program for the oven was as follows: 45 °C for 4 min, heating with 3 °C/min to 280 °C followed by 20 min at 280 °C. Helium was used as the carrier gas with a constant flow rate of 2 ml/min.

Solubility test. Solubility tests were performed by mixing 1 g of pyrolysis oil or upgraded oil with 2 g of a mixture of *n*-hexane and benzene (1 to 1 wt ratio) in a 10 ml test tube. The mixture was then stirred in an ultrasonic bath for 5 min, subsequently heated to 40 °C for 30 min, and allowed to phase separate overnight at room temperature. Both layers were weighted. The top phase was shown to be rich in *n*-hexane and benzene. The solubility of the upgraded oil in the hexane–benzene mixture was estimated using the following equation:

$$\text{solubility} = \frac{m_{\text{HB rich layer}} - m_{\text{HB initial}}}{m_{\text{HB initial}}} \left(\frac{g_{\text{oil}}}{g_{\text{HB}}}\right) \quad (5)$$

where $m_{\text{HB rich layer}}$ is the mass of the hexane–benzene rich layer after equilibration and $m_{\text{HB initial}}$ the mass intake of the hexane–benzene mixture.

Capillary electrophoresis. A capillary electrophoresis (CE) system from Agilent Technologies was used to determine the amount of organic acids in the upgraded oil. The CE apparatus was equipped with a standard fuse capillary (75 μm i.d., 72 cm active length, and 80.5 cm total length) and a diode array detector (DAD). The CE was operated at 20 °C and a voltage of −25 kV. Electropherograms were recorded in DAD at 350 nm with a reference at 200 nm. A buffer solution (pH 4.6) from Agilent Technologies containing 5 mM cetyltrimethyl-ammonium bromide (CTAB) was used. The

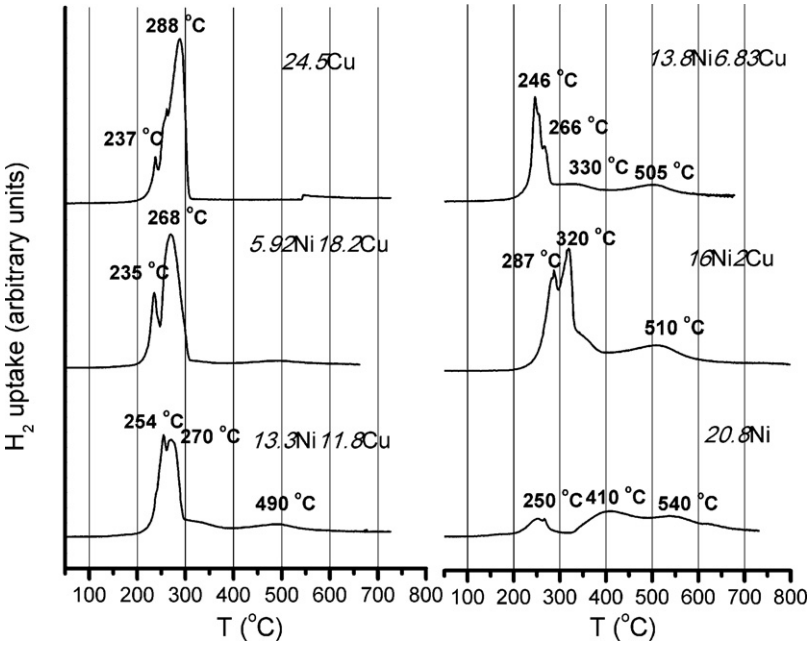

Fig. 1. H_2–TPR curves of monometallic Cu and Ni catalysts and bimetallic Ni-Cu catalysts.

capillary was preconditioned prior to each measurement by flushing the buffer solution for 4 min at 1 bar.

ICP-OES (inductively coupled plasma-optical emission spectrometry). The metal content in the aqueous phase after reaction was determined using ICP using an Optima 700 DV (PerkinElmer) analyzer.

2.5.2. Catalyst performance indicators for hydrotreatment experiments with fast pyrolysis oil

The H_2 consumption for each experiment (4 h) was determined to calculate the catalyst activity. It is based on pressure and temperature recordings and composition data before and after the reaction. Details about the calculation procedure are given in Supplementary information. The activity of the catalyst is calculated from the H_2 uptake during reaction (4 h), catalyst intake (Eq. (6)) and expressed as $NL_{hydrogen}/(kg_{PO}\, g_{active\ metal})$. For the bimetallic complexes, the activity is based on the sum of the amount of the active metals (Ni and Cu) in the catalyst formulation.

$$\text{Catalyst activity} = \frac{H_2\ \text{uptake}}{g_{\text{active metal}}}\,(NL_{\text{hydrogen}}/(kg_{PO}\, g_{\text{active metal}})) \quad (6)$$

3. Results and discussion

3.1. Synthesis and characterization of the Ni-Cu on δ-Al_2O_3 catalysts

The catalysts were prepared by wet impregnation of the metals on a δ-Al_2O_3 support. An overview of the catalyst formulations used in this study is given in Table 2. The total loading of active metals (Ni and Cu, around 20 wt%) is about similar, though the Ni to Cu weight ratios varies considerably. For comparison, two monometallic catalysts (Ni/δ-Al_2O_3 and Cu/δ-Al_2O_3) were prepared and tested as well. These may be regarded as extremes with respect to metal composition.

The reduction temperature of the supported catalysts was determined with TPR, and the results are given in Fig. 1. For the monometallic Cu catalyst (24.5Cu), a single reduction temperature at 288 °C was observed. For monometallic Ni (20.8Ni) three peaks at about 250, 410, and 540 °C were present, representing Ni (III) oxide reduction [35,36], reduction of Ni(II) to Ni(0) species and reduction of surface $NiAl_2O_4$ species, respectively.

The TPR curves of the mono- and bimetallic catalysts differ considerably and the bimetallic catalysts are more readily reduced than monometallic Ni. For instance, the high temperature peak in the TPR for monometallic Ni (reduction of $NiAl_2O_4$) is at higher temperature than for bimetallic catalysts. The position of this peak for the latter catalysts depends on the copper content, with higher Cu contents leading to a lower reduction temperature (c.f. 510 °C for16Ni2Cu and 490 °C for 13.3Ni11.8Cu). TPR spectra of the bimetallic catalysts also show sharp peaks at temperatures below 320 °C. This indicates that promotion of Ni catalysts with Cu leads to a considerable reduction of the temperature for the transition of Ni(II) to metallic Ni(0).

XRD was applied to observe the change of oxidation states during reduction, to measure the lattice parameter of δ-Al_2O_3 (Fig. 3), and to investigate the metal phase composition (Table 6). To gain insights in the changes in oxidation states during reduction, characterization by in situ high temperature XRD (300 °C, 10 bar hydrogen) was performed, and the results were compared with freshly prepared catalysts (Fig. 2) and the δ-Al_2O_3(support. For the Ni-only catalyst (20.8Ni), the XRD patterns before and after reduction at 300 °C were similar. This indicates that considerable reduction does not occur at 300 °C, in agreement with the TPR data (Fig. 1). The XRD pattern of the 24.5Cu after reduction differs from the original sample and only peaks for Cu(0) are present. This is

Table 2
Overview of the catalysts used in this study.[a]

Catalyst	Metal loading (wt%)	
	Ni	Cu
20.8Ni	20.80	–
16Ni2Cu	16.00	2.00
13.8Ni6.83Cu	13.80	6.83
13.3Ni11.8Cu	13.30	11.80
5.92Ni18.2Cu	5.92	18.20
24.5Cu	–	24.50

[a] Catalyst support is δ-Al_2O_3.

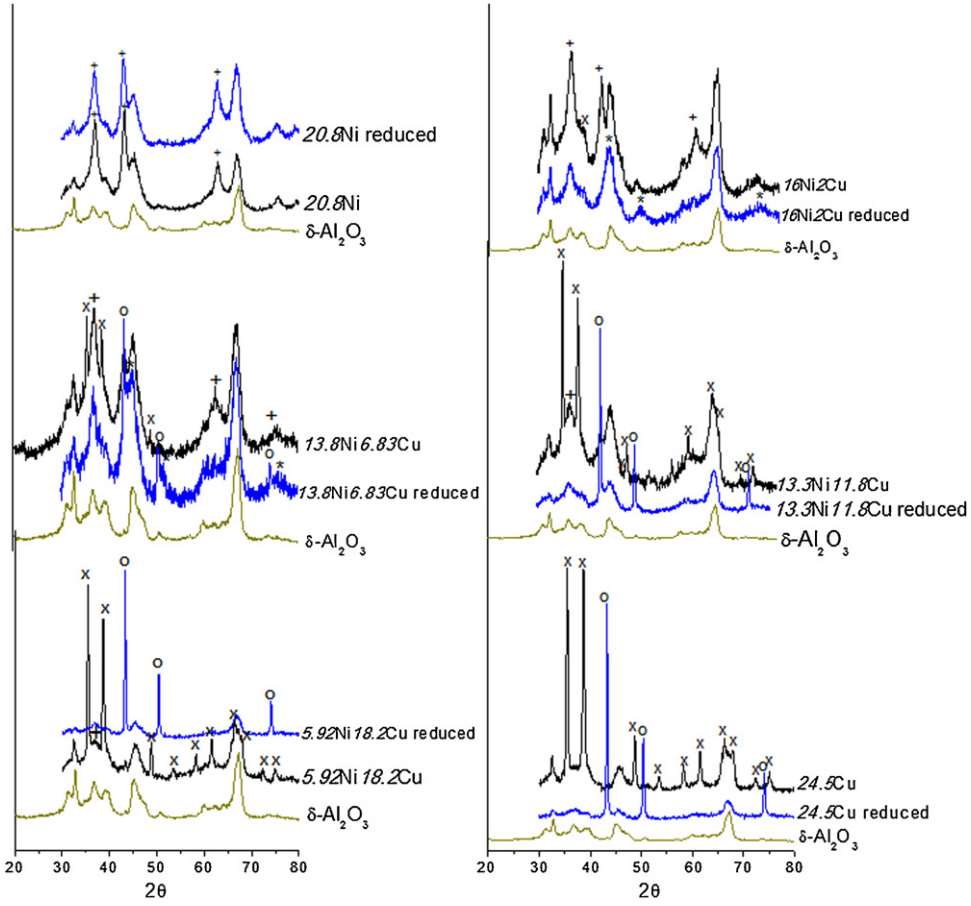

Fig. 2. XRD patterns of Ni/δ-Al_2O_3, Cu/δ-Al_2O_3 and the bimetallic Ni-Cu/δ-Al_2O_3 catalysts, ○: Cu(0); ×: CuO; *: Ni; +: NiO, after preparation and after reduction at 300 °C.

indicative for complete reduction below 300 °C, in line with the TPR data.

For bimetallic catalysts, the extent of reduction is a function of the Ni to Cu ratio in the samples. For the lowest ratio (16Ni2Cu), several Ni(0) peaks appeared after reduction, but peaks for Cu(0) could not be clearly observed. However, NiO peaks are still present in the reduced samples, indicating that reduction of 16Ni2Cu is not complete at 300 °C (see Fig. 2). For catalysts with higher Cu contents (13.8Ni6.83Cu), also the Cu(0) peaks appeared. For samples with even higher Cu levels (13.3Ni11.8Cu and 5.92Ni18.2Cu), Ni(II) peaks is absent after reduction, indicating that both Ni and Cu were reduced to a considerable extent.

The δ-Al_2O_3 support was calcined in air at 1000 °C before impregnation. This treatment may lead to a phase transition to α-Al_2O_3. The absence of clear peak at 2θ values around 22°, characteristic for the (0 1 2) plane of α-Al_2O_3 indicates that phase transition did not occur during calcination [37].

The lattice parameter of the δ-Al_2O_3 support for the different catalysts is shown in Fig. 3. It is a function of the Ni content and increases at higher contents. This can be explained by the higher diffusion rates of Ni in the alumina support, and possibly also the formation of higher amounts of Ni spinels ($NiAl_2O_4$) at higher Ni intakes. The formation of surface Ni spinels is expected to have possible positive and negative effects on catalyst activity. It leads to stronger interactions of the active component with the support, which is expected to keep the active component in a dispersed state and as such reduce the tendency for agglomeration. On the other hand, Ni spinels are more difficult to reduce than other Ni species and therefore reduce the formation rate of active Ni(0) [26,38]. The addition of copper to Ni/Al_2O_3 has previously reported to prevent the formation or growth of $NiAl_2O_4$ spinels.

3.2. Catalytic hydrotreatment reactions of anisole using bimetallic Ni-Cu catalysts on δ-Al_2O_3

Anisole was selected as a model component as phenolic compounds are known to be among the most persistent compounds in catalytic hydrotreatment reactions of fast pyrolysis oil [17]. Thus, catalysts with good performance for anisole are likely also good

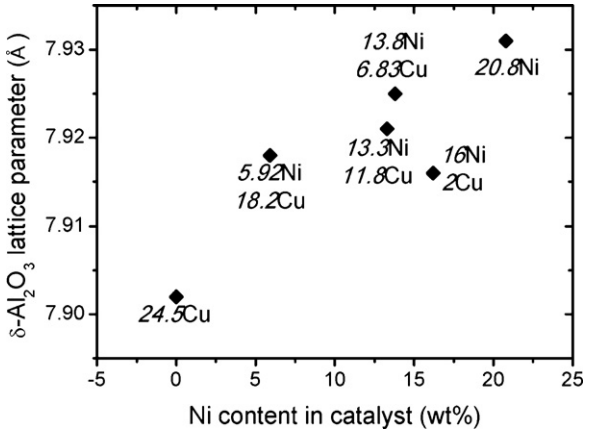

Fig. 3. Lattice parameter of δ-Al_2O_3 versus Ni content in the catalyst.

Table 3
Overview of results for the hydrotreatment of anisole at 300 °C with Ni-Cu/δ-Al_2O_3 catalysts.

Catalyst	Anisole conversion (X_A) (mol%)	HDO selectivity (mol%)	Yield of oxygen-free products (mol%)	Specific catalytic activity (mol s^{-1} g active metals^{-1} × 10^7)
Quartz	2.8	0	0	–
Al_2O_3	11.8	0	0	–
20.8Ni	66.1	97.8	64.6	5.0
16Ni2Cu	78.6	95.9	75.4	7.3
13.8Ni6.83Cu	73.8	90.6	66.9	6.4
13.3Ni11.8Cu	70.3	82.8	58.2	6.1
5.92Ni18.2Cu	76.9	72.8	56.0	6.9
24.5Cu	95.3	1.0	1.0	0.2

candidates for further testing with actual fast pyrolysis oil [32,39]. The reactions were carried out in a packed bed reactor operated in a continuous mode at a temperature of 300 °C in combination with WHSV values between 3 and 6 h^{-1}. For comparison, quartz and δ-Al_2O_3 were tested as well. The experimental results are summarized in Tables 3 and 4.

Mono- and bimetallic catalysts are both active in anisole deoxygenation, with conversions between 66.1 and 95.3 mol%. Quartz and the alumina support alone showed limited activity. Anisole conversion for the bimetallic catalysts is within a narrow range of 70–80 mol%, and a trend as a function of the Ni-Cu ratio is not clear. The 16Ni2Cu is the most active in the series. The conversion for the monometallic Ni on δ-Al_2O_3 catalyst is considerably lower (66.1 mol%) than for bimetallic ones, which indicates a positive effect of Cu addition. The higher activity of the Ni-Cu catalysts compared to monometallic Ni may be attributed to reduced Ni spinel formation by the addition of Cu. This is supported by a lower δ-Al_2O_3 lattice parameters for the bimetallic Ni-Cu catalyst (Fig. 3), indicating that less Ni is incorporated in the Al_2O_3 structure and converted to inactive spinels when compared to monometallic Ni.

A number of compounds are formed upon the catalytic hydrotreatment reactions (Table 4). Typical oxygen free HDO products are benzene and toluene, and consecutive hydrogenation products thereof such as cyclohexane and methylcyclohexane. In addition, oxygenates as phenol, cyclohexanole and cyclohexanone are also present. These product compositions are in line with a reaction network proposed for the catalytic hydrotreatment of anisole using CoMo/γ-Al_2O_3 and MoO_3-NiO-A1$_2O_3$ catalysts [39].

The selectivity of the reaction is a strong function of the type of catalysts. For Cu only, though very active (95.3 mol% conversion), the degree of deoxygenation is very low (1%) and the main products are phenol and methylphenols. Some methane is formed as well (around 2% of feed). Reaction with the monometallic Ni catalyst gives the highest HDO selectivity (97.8%), but a low conversion of anisole (66 mol%). Here, the main product is benzene.

For bimetallic catalysts, the HDO selectivity is between 70 and 96%, the main products are benzene and cyclohexane. The HDO selectivity is a function of the Ni content, with a higher Ni content (and a concomitant lowering of the Cu content) showing higher HDO selectivities. In addition, the aliphatic/aromatic hydrocarbon product ratio is a strong function of catalyst composition (Fig. 4). The aliphatic content is higher for the bimetals than for the monometallic Ni, indicating that Ni-Cu catalysts are more active for the hydrogenation of the aromatic rings than the monometallic ones. This effect may be associated with the amount of active $Ni_{1-x}Cu_x$ metal clusters, as such clusters are known to be more active for the hydrogenation of aromatics than the individual monometallic catalysts.

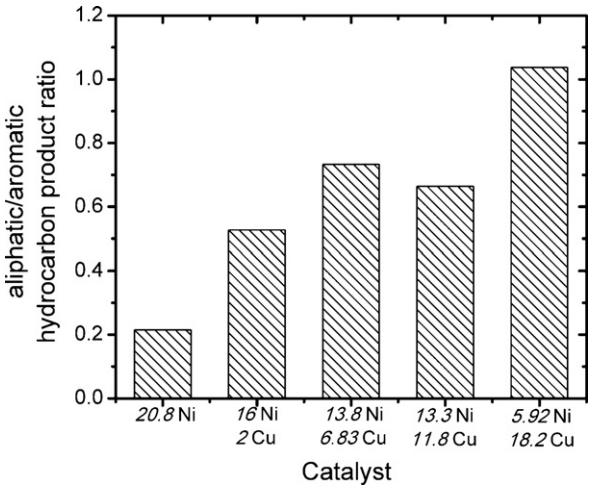

Fig. 4. Aliphatic and aromatic hydrocarbon product ratio versus catalyst composition for the hydrotreatment of anisole at 300 °C.

3.3. Catalytic hydrotreatment of fast pyrolysis oil using Ni/Cu on δ-Al_2O_3 catalysts

The catalytic hydrotreatment of fast pyrolysis oil with the bimetallic Ni/Cu on δ-Al_2O_3 catalysts was performed in a batch autoclave at an initial pressure of 100 bar (at RT) using a standardized heating up temperature profile (150 °C for 1 h, followed by 350 °C for 3 h). This 2-stage heating profile was shown to reduce coke formation [5]. The results were compared with data obtained for Ru/C, the latter has been studied extensively for fast pyrolysis oil upgrading [2,20,23–25,40].

Table 4
Product selectivity for the hydrotreatment of anisole at 300 °C with Ni-Cu/δ-Al_2O_3 catalysts.

Catalyst	Quartz	Al_2O_3	24.5Cu	5.92Ni18.2Cu	13.3Ni11.8Cu	13.8Ni6.83Cu	16Ni2Cu	20.8Ni
Cyclohexane	0	0	0	29.2	27.7	32.8	24.3	14.9
Benzene	0	0	0	28.6	42.2	43.5	59.9	72.5
methylcyclohexane	0	0	1.0	7.8	5.3	5.5	8.8	2.4
Toluene	0	0	0	7.1	7.5	8.8	2.9	8.1
Cyclohexanole	0	0	0	0	2.3	5.9	2.3	0
Cyclohexanone	0	0	0	2.7	0	0	1.8	0
Phenol	100	100	99	22.6	13.3	1.2	0	2.2
Other products	0	0	0	1.9	1.6	2.3	0	0

Table 5
Hydrogen consumption and mass balance for catalytic hydrotreatment of fast pyrolysis oil.[a]

Catalysts	20.8Ni	16Ni 2Cu	13.8Ni 6.83Cu	13.3Ni 11.8Cu	5.92Ni 18.2Cu	24.5Cu	Ru/C[b]
H_2 uptake (NL/kg_{PO})	58	146	138	122	100	64	272
							Yields(wetbasis)
Product oil (wt% of feed)	36.8	40.8	42.2	40.3	35.0	36.8	37.2
Aqueous phase, wt% of feed	32.1	42.7	41.8	30.6	25.8	33.1	43.7
Char (acetone insoluble) (wt% of feed)	1.3	0.6	2.2	3.2	3.9	2.0	1.13
Coke deposited on the catalyst (wt% of feed)[c]	1.0	0.4	0.9	0.7	0.7	0.7	n.d.[d]
Gas (wt% of feed)	5.1	7.2	7.5	7.8	11.5	10.7	11.2
Mass balance closure (wt%)	76	92	95	83	77	83	93
Oxygen content of organic phase (wt%, dry)	12.2	17.1	16.5	16.1	12.6	10.4	12.0
Moisture content of product oil (wt%)	7.2	4.1	4.4	4.7	7.1	9.6	2.0

[a] 150 °C (1 h) and 350 °C (3 h), with initial pressure of 100 bar at RT.
[b] Initial pressure of 120 bar at RT.
[c] Based on TGA data.
[d] Not determined.

3.3.1. Product formation and mass balances

The amounts of the various product phases after the reaction are provided in Table 5. When using the Ni-Cu catalysts, the liquid phase consisted of two separate phases, a bottom phase consisting of the product oil and a slightly yellowish aqueous top phase. For the Ru/C as benchmark, the organic product oil was always floating on top of the aqueous phase [20,24]. Mass balance closure for the experiments ranged between 76 and 95 wt%, see Table 5 for details. The lower values for some of the experiments are related to the high viscosity of the product oils, which tend to stick to the lines, reactor walls and inserts and are very difficult to collect. To test the reproducibility, two experiments were carried out using the 16Ni2Cu catalyst at standard conditions. The hydrogen uptake was 136 and 146 NL/kg PO (7% difference) for both experiments, whereas the H/C ratio of the organic phase was 1.36 and 1.41 (4% difference). The oil yields are 41 and 38 wt% for both experiments. These reproducibility data are in line with earlier detailed experimental studies carried out in our group in the current batch set-up for Ru/C catalysts [20,23,24], also an indication that reproducibility is satisfactorily.

The yield of the product oil obtained over Ni-Cu catalysts was typically between 35 and 42 wt%. Hydrotreatment reactions with the reference Ru/C catalyst gave a yield of 37.2 wt%, which is in the range for the Ni-Cu catalysts. Of the carbon present in the fast pyrolysis oil feed, most ends up in the upgraded oil (64–75 wt%), whereas by far lower amounts are present in the aqueous (5–9 wt%), gas (3–8 wt%) and solid (char) phase (0.2–6 wt%).

The gas composition after reaction and the total amount of gas phase components formed during the reaction are summarized in Fig. 5. The product gas mainly consists of CO_2 (0.6–1.6 mmol/g feed), while some CH_4, CO, and smaller hydrocarbons (C_2–C_3) are present as well. The amount of product gases seems to increase slightly when increasing the Cu content in the catalyst. In comparison, Ru/C gave the highest amount of gases (10.7 wt%). Particularly the amount of CH_4 (1.1 mmol/g feed) is ten times more than for the Ni-Cu catalysts (0.05–0.1 mmol/g feed), and it appears that the Ni-Cu catalysts are by far less active in methanation reactions than Ru/C, which is positive regarding the (economic) incentive to reduce the hydrogen usage for the hydrotreatment process.

The amount of char formed during the reaction was between 0.6 and 3.9 wt% for the bimetallic catalysts. A clear trend between the amount of char and catalyst composition is absent.

The activity of the catalysts, as calculated from the H_2 uptake, is given in Fig. 6. This figure shows that the 16Ni2Cu catalyst is the most active in the series. Thus, activity is the highest for the catalyst with the highest Ni content (Fig. 6). The bimetallic catalysts are more active than the monometallic ones, an indication for a synergic effect between Ni and Cu. The uptake for the Ru/C catalyst on the other hand was considerably higher than for the Ni-Cu catalysts (272 NL/kg PO).

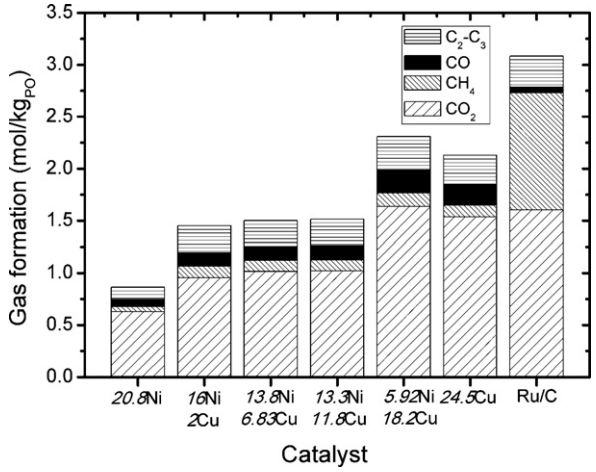

Fig. 5. Gas production and composition for the hydrotreatment of pyrolysis oil with Ni-Cu based catalysts and a commercial Ru/C catalyst at 150 °C (1 h) and 350 °C (3 h), with initial pressure of 100 bar at RT (120 bar for Ru/C).

The higher activity of the bimetallic catalyst compared to the monometallic catalyst is in agreement with the result for the HDO of anisole (Table 3), and it is partially attributed to the higher reducibility of the bimetallic catalysts as shown by the TPR (Fig. 1).

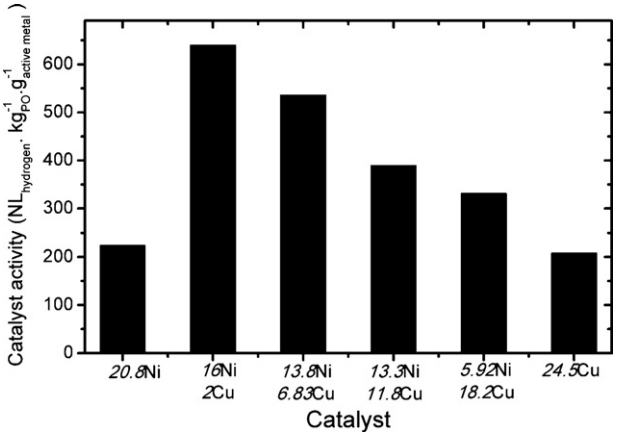

Fig. 6. Catalyst activity based on the H_2 uptake. Conditions: 150 °C (1 h) and 350 °C (3 h), with initial pressure of 100 bar at RT (120 bar for Ru/C).

Table 6
Phase composition of the fresh (before reduction) and spent catalysts (after hydrotreatment of pyrolysis oil at 150 °C (1 h) and 350 °C (3 h), with initial pressure of 100 bar at RT (120 bar for Ru/C).

Sample	Phase composition (CSD size, Å)	
	Oxidized, before reaction	After reaction
20.8Ni	NiO (90) Al_2O_3	Ni (250) Al_2O_3
16Ni2Cu	CuO (n.d.)[b] NiO (60) Al_2O_3	Cu traces $Ni_{0.85}Cu_{0.15}$ (230) Al_2O_3
13.8Ni6.83Cu	CuO (340) NiO (50) Al_2O_3	Cu (190) $Ni_{0.75}Cu_{0.25}$ (150) Al_2O_3
13.3Ni11.8Cu	CuO (410) NiO traces Al_2O_3	Cu (230) $Ni_{1-x}Cu_x$ (140)[a] Al_2O_3
5.92Ni18.2Cu	CuO (400) Al_2O_3	Cu (350) Ni traces Al_2O_3
24.5Cu	CuO (440) Al_2O_3	Cu (450) Al_2O_3

[a] Exact composition could not be determined.
[b] n.d.: not clearly detectable.

Moreover, XRD also indicates the formation of various Ni_xCu_{1-x} clusters after reaction (Table 6). This has been observed before by Rogatis et al. [41], although separate Ni and Cu particles were not reported by them, probably due to the low total loading of Ni and Cu in their work. The Ni_xCu_{1-x} clusters are most likely the actual active phase for the catalytic hydrotreatment reaction. Unfortunately, clear relations between the XRD data and the activity of the various catalysts are absent. However, as will be demonstrated later, the best catalyst in the series (16Ni2Cu) also shows the lowest level of leaching and coke deposition and, besides differences in amount and size of the active Ni_xCu_{1-x} clusters, these factors likely also affect catalyst activity.

3.3.2. Elemental composition of the upgraded oil

The oxygen content of the upgraded oils ranges between 10.4 and 17.1 wt% (dry basis), which is much lower than the original fast pyrolysis oil (40.1 wt%, dry basis). This is partly due to a considerable reduction in the water content, 4.1–9.6 wt% for the upgraded oils (Table 5) versus 23.9 wt% for the fast pyrolysis oil feed (Table 1).

The elemental compositions of the product oils are presented in a Van Krevelen plot, see Fig. 7 for details. The O/C ratios for all product oils fall within a rather narrow range (0.08–0.17). However, a significant spread in the H/C ratios (1.0–1.6) is observed. For the

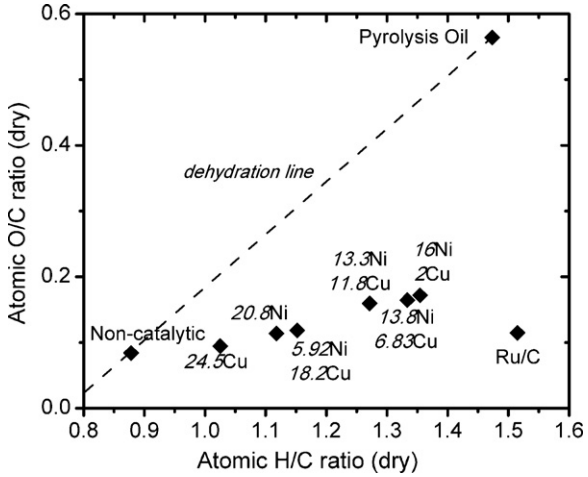

Fig. 7. Van Krevelen plot for the organic product phases (dry bases). Upgraded oils are obtained from hydrotreatment at 150 °C (1 h) and 350 °C (3 h), with initial pressure of 100 bar at RT (120 bar for Ru/C).

Ni-Cu catalysts, the highest H/C ratio was obtained for 16.2Ni2Cu (1.35), but this is still considerably lower than for Ru/C. Catalytic hydrotreatment with monometallic Cu catalyst (24.5Cu) resulted in upgraded oil with the lowest H/C ratio, whereas the H/C ratio was slightly higher when the monometallic Ni catalyst (20.8Ni) was used. The H/C ratio correlates nicely with the hydrogen uptake (Table 5) and a high hydrogen uptake leads to product oils with a high H/C ratio. For comparison, the composition of a product oil obtained in the absence of a catalyst ('thermal process') is also presented. In this case, the product oil is a very viscous nearly solid paste with very low H/C (0.88) and O/C (0.08) ratios. This thermal pathway has been studied in detail [42,43] and the low H/C and O/C ratios are rationalized by assuming the occurrence of a variety of dehydration reactions leading to the formation of water.

3.3.3. Molecular composition of the product oils

To gain insights in the molecular composition of the product oils the samples were subjected to GC–MS/FID analyses (Table 7). Unfortunately, less than 20 wt% of components in the product oils were detected by GC, as this technique only provides information on the amounts of low molecular weight volatile compounds. The product oils contain considerable amounts of higher molecular weight compounds (for instance lignin fragments and oligomeric sugars), as shown by GPC measurements (vide infra). However, the GC data clearly show that low molecular weight sugars (such as levoglucosan) and smaller aldehydes (such as hydroxyacetaldehyde)

Table 7
Composition of pyrolysis oil and upgraded oils (in wt%, wet) by GC–MS/FID.[a]

Substance group	Pyrolysis oil	Catalyst						
		20.8Ni	16Ni 2Cu	13.8Ni 6.83Cu	13.3Ni 11.8Cu	5.92Ni 18.2Cu	24.5Cu	Ru/C
Acids	3.12	2.73	5.57	4.94	3.58	3.03	1.96	5.98
Nonaromatic alcohols			0.03	0.03				0.34
Nonaromatic aldehydes	6.06	–	–	–	–	–	–	–
Nonaromatic ketones	2.25	2.91	7.16	6.74	4.93	3.93	2.41	4.07
Furans		0.18	0.49	0.32	0.35	0.23	0.11	2.02
Sugars	2.53	–	–	–	–	–	–	–
Lignin derived phenols		1.22	1.46	1.55	1.00	1.84	1.29	2.69
Guaiacols (methoxy phenols)	2.03	2.08	2.51	2.32	1.94	2.07	1.60	4.83
Alkanes		0.03	0.07	0.06	0.31	0.03	0.03	7.19
Miscellaneous	0.10	0.27	0.45	0.46	1.04	0.46	0.28	1.05
Total identified	16.09	9.43	17.74	16.41	13.14	11.20	7.69	28.15

[a] The upgraded oils were obtained oils from hydrotreatment at 150 °C (1 h) and 350 °C (3 h), with initial pressure of 100 bar at RT (120 bar for Ru/C). 150 °C (1 h) and 350 °C (3 h), at a total pressure of 20 MPa at 350 °C.

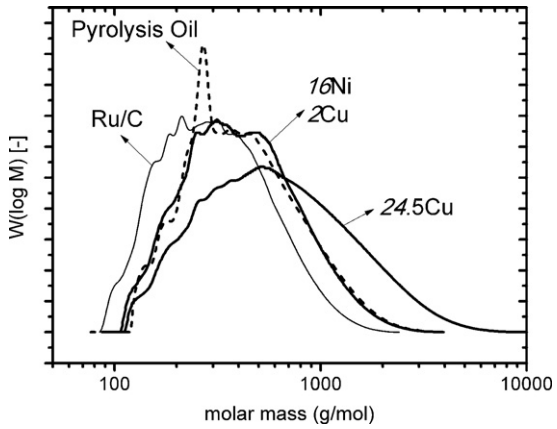

Fig. 8. GPC of upgraded oils using the 16Ni2Cu, 24.5Cu, and Ru/C catalysts. Upgraded oils are obtained from hydrotreatment at 150 °C (1 h) and 350 °C (3 h), with initial pressure of 100 bar at RT (120 bar for Ru/C).

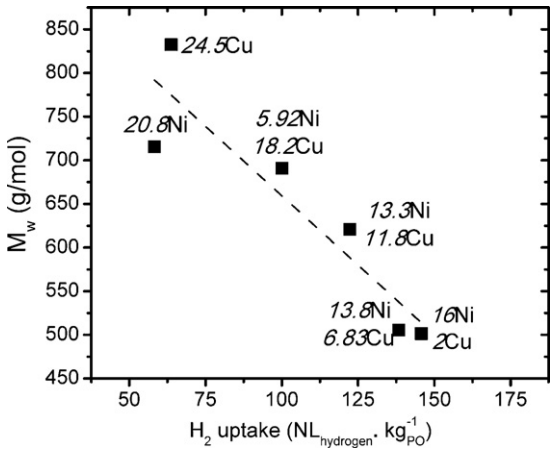

Fig. 9. Mass-average molecular weight (M_w) of the upgraded oils as a function of H_2 uptake during hydrotreatment. Upgraded oils are obtained from hydrotreatment at 150 °C (1 h) and 350 °C (3 h), with initial pressure of 100 bar at RT (120 bar for Ru/C).

are completely converted during the catalytic hydrotreatment reaction, independent of the catalyst used. This implies that these compounds are very reactive at the conditions employed. A slight increase in the amount of lignin derived phenolics is observed, indicating that high-molecular lignin fragments are broken down to its low molecular weight phenolics. Ru/C, the most active catalyst in this study (based on H_2 uptake, see Table 5), produces considerable amounts of alkanes.

3.3.4. Product properties of the product oils

Relevant product properties of (upgraded) pyrolysis oils when considering co-feeding in existing oil refinery units are viscosity, thermal stability, solubility in hydrocarbons and acidity. The viscosities of the upgraded oils obtained with some representative bimetallic catalysts were determined and found to be about 200–300 cP (225 for16Ni2Cu and 297 cP for 13.8Ni6.83Cu). These values are considerably higher than for the benchmark Ru/C catalyst (25 cP) and the fast pyrolysis oil feed (46 cP). An important contributor to these differences is likely the large spread in water content between the feed and product oils. Pyrolysis oils contain considerable amounts of water (up to 30%, and 23.9% for the oil used in this study), leading to relatively low viscosities. The phase separated upgraded product oils contain by far less water (4.1–9.6 wt%, see Table 5), leading to higher viscosities. In addition, the formation of higher molecular weight fragments during catalytic hydrotreatment may also contribute to a higher viscosity.

To test the latter hypothesis, the molecular weight distributions of the product oils were determined using GPC. Representative examples of GPC spectra are given in Fig. 8. For the bimetallic catalyst, the M_w values ranged between 500 and 690 g/mol, while the values are higher (720 g/mol for Ni and 830 g/mol for Cu) for the monometallic catalysts. For Ru/C, the lowest value was found (370 g/mol).

The viscosity correlates with the molecular weights of the products and higher viscosity is associated with a higher molecular weight. Interestingly, there also appears to be a relation between the molecular weight of the upgraded products and the hydrogen uptake during an experiment (Fig. 9). In the case of high hydrogen uptakes (high catalyst activity), the molecular weight of the product is reduced.

These findings may be rationalized by considering a reaction network recently established by Venderbosch et al. [25] for the hydrotreatment reaction using Ru/C (Scheme 1). In the initial phase of the hydrotreatment process, catalytic hydrogenation and thermal, non-catalytic repolymerization occur in a parallel mode. Repolymerization leads to the formation of soluble higher molecular weight fragments which upon further condensation reactions give char. This route is as such not preferred and the rate of the polymerization reactions should be reduced as much as possible. The preferred pathway involves hydrogenation of the thermally labile components in the pyrolysis oil feed to stable molecules that are not prone to polymerization. Subsequent reactions (hydrogenations and hydrocracking) on a time scale of hours lead to products with reduced oxygen contents and ultimately to higher H/C ratios. The relative rates of both pathways will eventually determine the ultimate product properties. The hydrogenation pathway is more dominant for reactions with a high hydrogen uptake, leading to low viscous products with a low molecular weight. The experimental findings for the Ni-Cu catalyst are in line with this pathway proposal and the experiments with the highest hydrogen uptake lead to products with the lowest M_w and highest H/C ratio.

To gain insights in the thermal stability of the product oils, defined in terms of the tendency of the products for coking, the product oils were subjected to TGA analyses. This may be considered as an alternative method for the well-established MCRT and CCR methods [44,45]. An example of a representative TGA profile is given in Fig. 10. The residue after heating to 900 °C under nitrogen

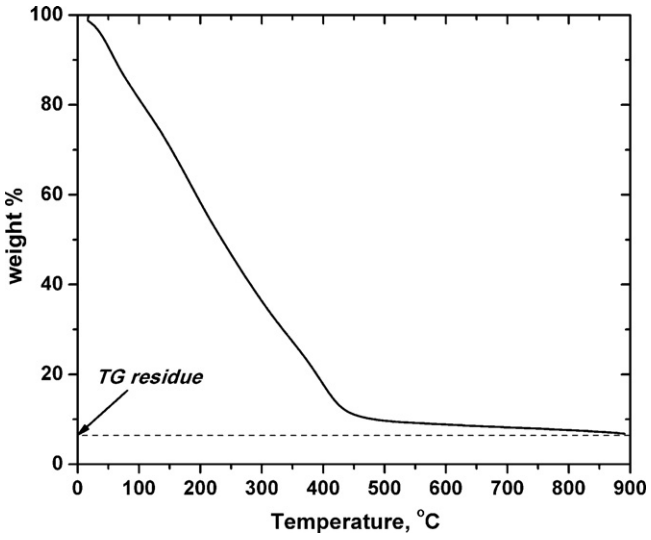

Fig. 10. TGA profile of upgraded oil obtained from hydrotreatment with 16Ni2Cu at 150 °C (1 h) and 350 °C (3 h), with initial pressure of 100 bar at RT (120 bar for Ru/C).

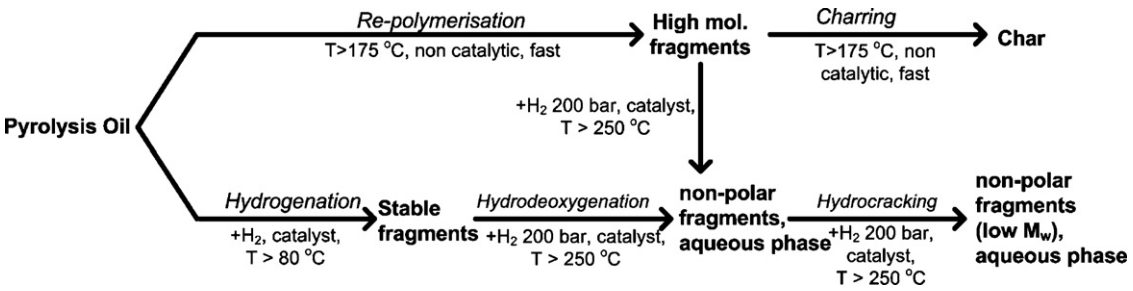

Scheme 1. Proposed pathways for the hydrotreatment of pyrolysis oil [25].

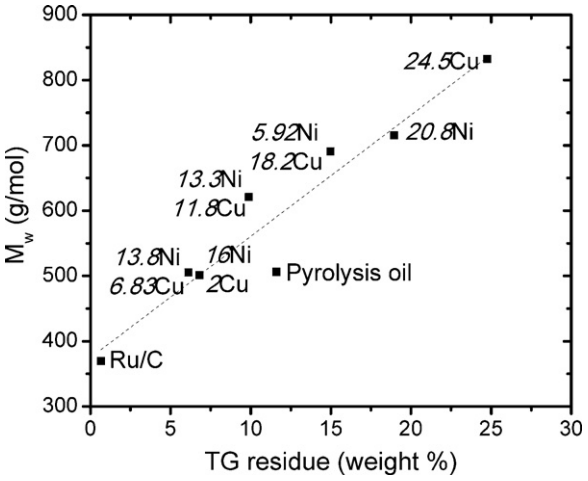

Fig. 11. TG residues versus the M_w of the upgraded oils. Upgraded oil is obtained from hydrotreatment at 150 °C (1 h) and 350 °C (3 h), with initial pressure of 100 bar at RT (120 bar for Ru/C).

(TG) is taken as a measure for the coking tendency. The TG value for the pyrolysis oil feed was 11.6 wt% and between 7.6 and 16.5 wt% for product oils obtained using the bimetallic Ni-Cu catalysts. The lowest values were observed for 13.8Ni6.83Cu and 16Ni2Cu, viz. catalysts with the highest hydrogen uptake during an experiment (Fig. 11). The TG residues for the monometallic Ni or Cu catalysts are considerably higher (19.0 wt% for Ni and 24.8 wt% for Cu). In comparison, the lowest value is observed for Ru/C, which is not surprising when considering the high hydrogen uptake for this catalyst (272 NL/kg_{PO}, Table 5).

The TG residue and the molecular weight of the product oils are related (see Fig. 11), and product oils with a lower molecular weight show lower values for the TG residues. A similar trend was earlier observed for catalytic hydrotreatment experiments of fast pyrolysis oil with a Ru/C catalyst [46]. It implies that the M_w is a good indicator for the coking tendency of the product oil. It is well possible that the higher molecular weight tail in the molecular weight distribution consists of large condensed molecules that are poorly volatile at temperatures at the upper limit of the TGA experiment (900 °C) and lead to higher TG residues. The experiments with the highest hydrogen uptake yield product oils with the lowest molecular weight and the highest H/C ratio, which can be rationalized by considering the competing pathways shown in Scheme 1.

The solubility of the upgraded oil obtained with the most active catalyst (16Ni2Cu) in hydrocarbons was estimated by mixing the product oil with an equimass mixture of n-hexane and benzene at room temperature. About 53 wt% of the upgraded oil dissolved in the n-hexane–benzene mixture, compared to only 4 wt% for the fast pyrolysis oil feed. Thus, the polarity of the product oil is reduced considerably upon the hydrotreatment reaction with the Ni-Cu catalysts and the solubility in typical hydrocarbons increases. Better results were obtained with the Ru/C benchmark catalyst and the product oil was completely soluble in the hydrocarbon mixture. This product has a higher H/C ratio, a lower TG residue and a higher content of aliphatic hydrocarbons (Table 7) and these factors likely render the oil more soluble in hydrocarbons.

The upgraded oils still contain substantial amounts of organic acids (2.73–5.98 wt%, Table 7), and the content is similar or, surprisingly, even higher than in the fast pyrolysis oil feed. It suggest that organic acids are very persistent for catalytic hydrotreatment, which was confirmed earlier for acetic acid [46], but also that organic acids are likely formed during the catalytic hydrotreatment reaction. The latter may be due to thermal decomposition reactions of the carbohydrate fraction in pyrolysis oil [47–49] or hydrogenated product thereof, which are known to produce considerable amounts of acids.

High product acidity is not recommended to avoid corrosion issues during co-feeding of the product oils in a refinery unit. Preliminary extraction experiments with water were performed to reduce the acid content of the product oils. The upgraded oil obtained using 16Ni2Cu was washed with water and subsequently both layers were separated. The organic acid content (acetic and formic acid) before and after washing was determined (capillary electrophoresis). Acetic acid reductions of up to 85% were observed (from 3.2 to 0.45 wt%) and formic acid could not even be detected in the product oil. Thus, these preliminary experiments indicate that a

Table 8
Metal content of the aqueous phases after reaction and extent of leaching.[a]

	Metal content in aqueous phase (ppm)			Extent of leaching (wt%)[b]		
	Ni	Cu	Al	Ni	Cu	Al
20.8Ni	125	<1	23	0.5	0	0.02
16Ni2Cu	48	<1	35	0.3	0	0.04
13.8Ni6.83Cu	95	21	94	0.6	0.3	0.11
13.3Ni11.8Cu	156	89	96	0.8	0.5	0.08
5.92Ni18.2Cu	319	362	60	2.9	1.1	0.04
24.5Cu	<1	<1	17	0	0	0.02

[a] Hydrotreatment performed at 150 °C (1 h) and 350 °C (3 h), with initial pressure of 100 bar at RT (120 bar for Ru/C).
[b] Defined as the amount of metal in the aqueous phase (g) divided by the intake of metal (g) times 100%.

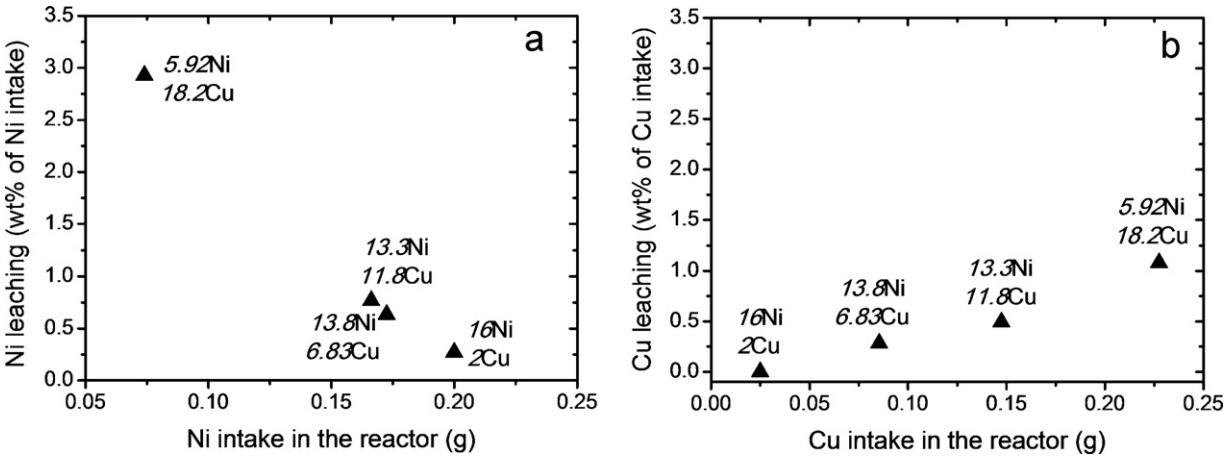

Fig. 12. Leaching of Ni (a) and Cu (b) as a function of the initial metal intake (hydrotreatment at 150 °C (1 h) and 350 °C (3 h).

simple waterwash could be an attractive option to reduce the acid contents in the product oils. Further research will be required to optimise extraction efficiencies and to assess the techno-economic potential of this extraction step.

3.4. Insights in catalyst structure before and after catalytic hydrotreatment reactions

To gain insights in the morphology, the amounts of active metals and carbon deposition a number of measurements (HRTEM, XRD, TGA) were performed on both fresh and used catalysts. Metal leaching was determined by analysing the aqueous phase after reaction with ICP (Table 8).

ICP-OES analyses show the presence of significant amounts of metals (Ni, Cu, and Al) in the aqueous phase, an indication for leaching of both the active metals and the support. The extent of leaching, defined as the amount of metal in the aqueous phase (g) divided by the intake of metal (g) times 100%, was in general lower than 1 wt%, with the exception of catalyst 5.92Ni18.2Cu (2.9% for Ni and 1.1% for Cu). The leaching order is Ni > Cu > Al. The low extent of leaching for 24.5Cu catalyst may be explained by agglomeration of the Cu phase during catalyst reduction and the hydrotreatment reaction. Moreover, hydrotreatment with monometallic Cu catalyst produced a high amount of char (vide infra, Table 9), which may limit the contact of the Cu particles with the acidic environment.

The extent of leaching of the bimetallic catalyst is a function of the metal intake, see Fig. 12 for details. The anticipated trend (higher leaching levels at higher intakes) is observed for Cu. Remarkably, the reverse is observed for Ni, and a higher Ni content on the supports for the bimetallic catalyst leads to lower leaching levels. A possible explanation is the acidity of the product oil, with a higher acidity leading to a higher tendency for metal leaching. However, this is not in line with the measured acid contents of the product oil, see Table 7 for details. The highest acid

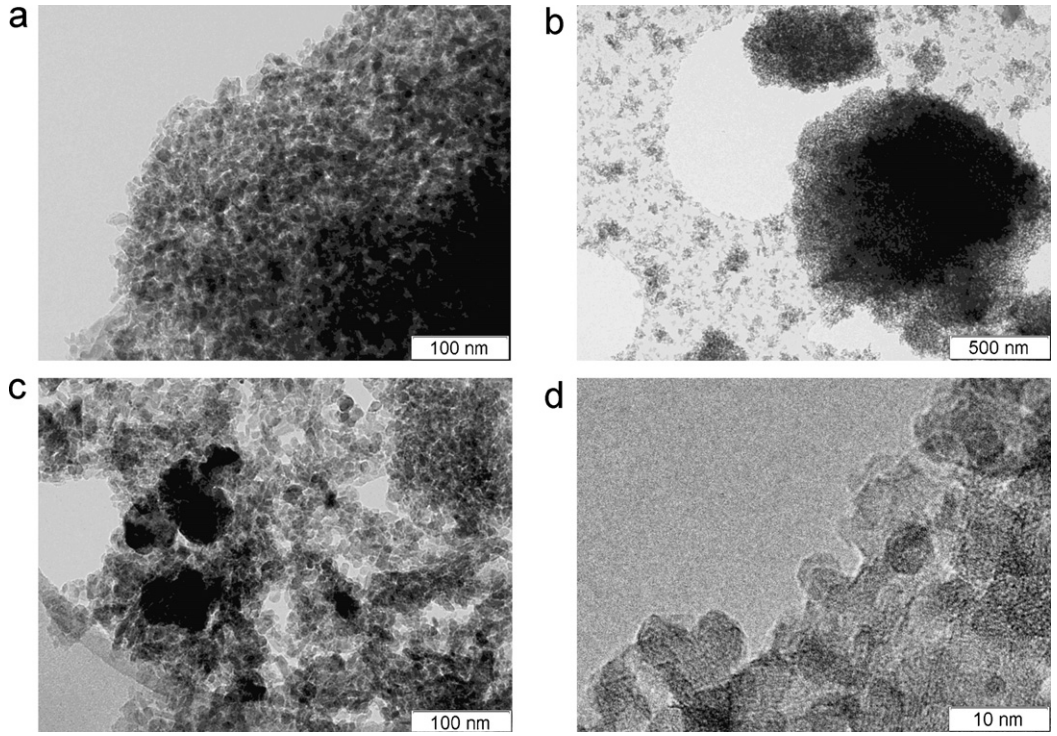

Fig. 13. HRTEM of 13.8Ni6.83Cu: (a and b) reduced at 300 °C, and (c and d) after hydrotreatment of pyrolysis oil at 150 °C (1 h) and 350 °C (3 h), with initial pressure of 100 bar at RT (120 bar for Ru/C).

Table 9
Carbon deposition on the catalyst after hydrotreatment of pyrolysis oil at 150 °C (1 h) and 350 °C (3 h), with initial pressure of 100 bar at RT (120 bar for Ru/C).

Catalyst	Carbon deposition (wt%)
20.8Ni	15.05
16Ni2Cu	8.90
13.8Ni6.83Cu	19.29
13.3Ni11.8Cu	15.65
5.92Ni18.2Cu	15.59
24.5Cu	24.45

contents were found for the oils produced using the catalyst with the highest Ni content (16Ni2Cu), and this catalyst shows the lowest leaching levels. The extent of leaching is also expected to be a function of the morphology of the active nickel-copper particles on the support and particularly on the surface area and the extent of reduction. In this respect, smaller particles and a lower extent of reduction (more oxidized, loosely bound metals) are expected to lead to higher leaching levels. Unfortunately, the XRD data of the spent catalyst (Table 6) do not provide sufficient information to draw definite conclusions on the observed leaching trend for Ni. Another possible explanation is the formation of larger amounts of Ni-spinels at higher Ni contents (Fig. 3). These spinels have strong interactions with the support and as such may lead to lower Ni leaching rates, with less Ni leaching at higher Ni intake as the result.

The HRTEM images of 13.8Ni6.83Cu catalyst before and after reaction are given in Fig. 13. The data indicate that the δ-Al_2O_3 support is stable at reaction conditions, which is also supported by XRD analyses (Table 6) after reaction. The HRTEM images indicate the occurrence of agglomeration of Ni and Cu-containing particles after reduction and the hydrotreatment reaction.

Carbon deposition on the alumina support was measured by performing TGA analysis on the spent catalysts in air and the results are given in Table 9. The amount of carbon on the catalysts is between 8.9 and 24.5 wt%. The highest carbon deposition was found for 24.5Cu, the lowest for 16Ni2Cu. This is in line with the activity data, where the latter was shown to be the most active in the series. Thus catalyst activity may among others also be related to coke deposition. Coke deposit on the bimetallic Ni-Cu catalysts is in general lower than for the monometallic Cu catalysts.

4. Conclusions

Bimetallic Ni-Cu catalysts with variable Ni-Cu contents on δ-Al_2O_3 were prepared and tested for the catalytic hydrotreatment of both anisole (a model compound) and fast pyrolysis oil. For both the hydrotreatment of anisole and fast pyrolysis oil, the bimetallic 16Ni2Cu catalyst appeared to be the most active and outperformed the monometallic Ni and Cu analogs. Catalyst activity is likely related to the size and amount of active Ni_xCu_{1-x} clusters in the catalyst formulation as well the extent of carbon deposit and metal leaching during the catalytic hydrotreatment reaction. The best NiCu catalyst is less active than the benchmark noble metal Ru/C catalyst, though is of particular interest due to the lower price of Ni compared to noble metal catalysts like Ru. In addition, metal leaching is an issue at the harsh reaction conditions for catalytic hydrotreatment and requires further research attention. Improved Ni based catalysts for the catalytic hydrotreatment reaction of fast pyrolysis oil have been prepared recently based on the insights obtained from this study and will be reported in due course.

Relevant product properties of the product oil considering co-feeding in existing oil refineries were determined. The thermal stability and particularly the coking tendency are improved considerably upon the hydrotreatment reaction and the product oils also show improved solubility in hydrocarbons. The viscosity was shown to be higher than the original pyrolysis oil feed, likely due to a lower water content and formation of some higher molecular weight components. Reduction of the viscosity is possible by blending with hydrocarbons. The acid content of the product oil is still considerable, though a water wash was found to be sufficient to reduce the acid levels considerably. Further research activities a.o. in labscale MAT units to determine the suitability of the product oils made using the bimetallic Ni-Cu catalysts for co-feeding in refinery units is in progress and will be reported in subsequent papers.

Acknowledgments

The authors would like to express their gratitude to Hans van der Velde and G.O.R. Alberda van Ekenstein (University of Groningen) for the EA, ICP-OES and TGA analyses, and C.B. Rasrendra (University of Groningen) for the CE analysis. Michael Windt and Dietrich Meier (von Thunen Institute, Hamburg) are acknowledged for recording and interpretation of the GC–MS/FID spectra. Finally, the BIOCOUP project (EU 6th framework project, contract number 518312) is acknowledged for financial support.

Appendix A. Supplementary data

Supplementary data associated with this article can be found, in the online version, at doi:10.1016/j.apcatb.2011.12.032.

References

[1] D. Chiaramonti, A. Oasmaa, Y. Solantausta, Renew. Sustain. Energy Rev. 11 (2007) 1056–1086.
[2] F. de Miguel Mercader, M.J. Groeneveld, S.R.A. Kersten, N.W.J. Way, C.J. Schaverien, J.A. Hogendoorn, Appl. Catal. B 96 (2010) 57–66.
[3] J.D. Adjaye, R.K. Sharma, N.N. Bakhshi, Fuel Process. Technol. 31 (1992) 241–256.
[4] R. Dimitrijevic, W. Lutz, A. Ritzmann, J. Phys. Chem. Solids 67 (2006) 1741–1748.
[5] J. Gagnon, S. Kaliaguine, Ind. Eng. Chem. Res. 27 (1988) 1783–1788.
[6] D.C. Elliott, E.G. Baker, Patent US Patent 4795841 (1989).
[7] S. Zhang, Y. Yan, T. Li, Z. Ren, Bioresour. Technol. 96 (2005) 545–550.
[8] C.N. Satterfield, S.H. Yang, J. Catal. 81 (1983) 335–346.
[9] C.-L. Lee, D.F. Ollis, J. Catal. 87 (1984) 332–338.
[10] E.O. Odebunmi, D.F. Ollis, J. Catal. 80 (1983) 65–75.
[11] E.O. Odebunmi, D.F. Ollis, J. Catal. 80 (1983) 76–89.
[12] C.-L. Lee, D.F. Ollis, J. Catal. 87 (1984) 325–331.
[13] O.I. Senol, T.R. Viljava, A.O.I. Krause, Catal. Today 100 (2005) 331–335.
[14] A.Y. Bunch, X. Wang, U.S. Ozkan, J. Mol. Catal. A: Chem. 270 (2007) 264–272.
[15] M. Ferrari, B. Delmon, P. Grange, Carbon 40 (2002) 497–511.
[16] S.K. Maity, M.S. Rana, B.N. Srinivas, S.K. Bej, G. Murali Dhar, T.S.R. Prasada Rao, J. Mol. Catal. A: Chem. 153 (2000) 121–127.
[17] E. Furimsky, Appl. Catal. A 199 (2000) 147–190.
[18] E. Laurent, B. Delmon, J. Catal. 146 (1994) 281–291.
[19] P.A. Horne, P.T. Williams, Renew. Energy 7 (1996) 131–144.
[20] J. Wildschut, F.H. Mahfud, R.H. Venderbosch, H.J. Heeres, Ind. Eng. Chem. Res. 48 (2009) 10324–10334.
[21] D.C. Elliott, J. Hu, T.R. Hart, G.G. Neuenschwander, Patent US Patent 7425657 (2008).
[22] A. Gutierrez, R.K. Kaila, M.L. Honkela, R. Slioor, A.O.I. Krause, Catal. Today 147 (2009) 239–246.
[23] J. Wildschut, I. Melián-Cabrera, H.J. Heeres, Appl. Catal. B 99 (2010) 298–306.
[24] J. Wildschut, M. Iqbal, F.H. Mahfud, I.M. Cabrera, R.H. Venderbosch, H.J. Heeres, Energy Environ. Sci. 3 (2010) 962–970.
[25] R.H. Venderbosch, A.R. Ardiyanti, J. Wildschut, A. Oasmaa, H.J. Heeres, J. Chem. Technol. Biotechnol. 85 (2010) 674–686.
[26] J.H. Sinfelt, J.L. Carter, D.J.C. Yates, J. Catal. 24 (1972) 283–296.
[27] P.G. Savva, K. Goundani, J. Vakros, K. Bourikas, C. Fountzoula, D. Vattis, A. Lycourghiotis, C. Kordulis, Appl. Catal. B 79 (2008) 199–207.
[28] L. De Rogatis, T. Montini, A. Cognigni, L. Olivi, P. Fornasiero, Catal. Today 145 (2009) 176–185.
[29] J.-H. Lee, E.-G. Lee, O.-S. Joo, K.-D. Jung, Appl. Catal. A 269 (2004) 1–6.
[30] O.V. Andryushkova, O.A. Kirichenko, V.A. Ushakov, in: A. Dabrowski (Ed.), Studies in Surface Science and Catalysis, Elsevier, 1999, pp. 587–619.
[31] Catal. Today 5 (1989) 1–120.
[32] V.A. Yakovlev, S.A. Khromova, O.V. Sherstyuk, V.O. Dundich, D.Y. Ermakov, V.M. Novopashina, M.Y. Lebedev, O. Bulavchenko, V.N. Parmon, Catal. Today 144 (2009) 362–366.
[33] A.L. Vishnevskii, V.V. Molchanov, T.A. Kriger, L.M. Plyasova, Proceedings of International Conference on Powder Diffraction and Crystal Chemistry, St. Petersburg, 1994.

[34] P. Scherrer, Nachrichten von der Gesellschaft der Wissenschaften zu Göttingen, Mathematisch-Physikalische Klasse 2 (1918) 98.
[35] B. Mile, D. Stirling, M.A. Zammitt, A. Lovell, M. Webb, J. Catal. 114 (1988) 217–229.
[36] V.N. Vorobjev, E.S. Svennitsky, G.S. Talipov, Kinet. Katal. 17 (1976) 208.
[37] A. Boumaza, L. Favaro, J. Lédion, G. Sattonnay, J.B. Brubach, P. Berthet, A.M. Huntz, P. Roy, R. Tétot, J. Solid State Chem. 182 (2009) 1171–1176.
[38] T.V. Reshetenko, L.B. Avdeeva, Z.R. Ismagilov, A.L. Chuvilin, V.A. Ushakov, Appl. Catal. A 247 (2003) 51–63.
[39] T.R. Viljava, R.S. Komulainen, A.O.I. Krause, Catal. Today 60 (2000) 83–92.
[40] J. Wildschut, J. Arentz, C.B. Rasrendra, R.H. Venderbosch, H.J. Heeres, Environ. Prog. Sustain. Energy 28 (2009) 450–460.
[41] L.D. Rogatis, T. Montini, B. Lorenzut, P. Fornasiero, Energy Environ. Sci. 1 (2008) 501–509.
[42] M. Rep, R.H. Venderbosch, D. Assink, W. Tromp, S.R.A. Kersten, W. Prins, in: A.V. Bridgwater, D.G.B. Boocock (Eds.), Science in Thermal and Chemical Biomass Conversion, CLP Press, 2006, pp. 1526–1535.
[43] F. d.M. Mercader, M.J. Groeneveld, S.R.A. Kersten, R.H. Venderbosch, J.A. Hogendoorn, Fuel 89 (2010) 2829–2837.
[44] P. Ghetti, Fuel 73 (1994) 1918–1921.
[45] F. Noel, Fuel 63 (1984) 931–934.
[46] A.R. Ardiyanti, R.H. Venderbosch, H.J. Heeres, Proceedings of 2009 AIChE Spring Annual Meeting, Tampa, 2009.
[47] Z. Srokol, A.G. Bouche, A. Van Estrik, R.C.J. Strik, T. Maschmeyer, J.A. Peters, Carbohydr. Res. 339 (2004) 1717–1726.
[48] B. Girisuta, B. Danon, R. Manurung, L.P.B.M. Janssen, H.J. Heeres, Bioresour. Technol. 99 (2008) 8367–8375.
[49] P.J. Oefner, A.H. Lanziner, G. Bonn, O. Bobleter, Monatsh. Chem. 123 (1992) 547–556.